Journal of Sound and Vibration (2001) **239**(3), 489–504
doi:10.1006/jsvi.2000.3142, available online at http://www.idealibrary.com on IDEAL®

TRANSIENT VIBRATION ANALYSIS OF A HIGH-SPEED FEED DRIVE SYSTEM

C. C. Cheng and J. S. Shiu

Department of Mechanical Engineering, National Chung Cheng University, Chia-Yi 621, *Taiwan, Republic of China*

(*Received* 21 *June* 1999, *and in final form* 12 *June* 2000)

The transient vibration of a high-speed feed drive system is investigated. In this study, an analogue vibratory equivalent model with multi-degree of freedom assembled with spring, mass and damper is used to simulate the dynamic behavior of a feed drive system. The worktable is capable of travelling at variable speed and can be brought to a halt at a desired position on the supporting structure. The focus is placed on the vibration response caused by the moving table subjected to different velocity motion programs. Results show that doubling the table moving speed raises more than four times of the table displacement at the moment that the table stops. A motion program with abrupt changes in the velocity and the acceleration should be avoided. Moreover, the symmetrical motion program leads to less vibration in the horizontal direction for the supporting structure.

1. INTRODUCTION

The function of mechanical feed drive system in a machine tool is to transmit the motion received from the feed motor to the table. A mechanical feed drive system comprises components such as servomotor, ball screw and a moving table that is mounted on a supporting structure. Because increased productivity has recently become a stringent necessity, demands of a high-speed feed drive system increase. These increases in speed demands were accompanied by constant requirements of improved machining accuracy. The position error of the table in a feed drive system is hindered not only by kinematic error but also by dynamic behavior of components due to acceleration forces and friction. With the increased demands in performance, considerable vibration problems become apparent. Vibrations are undesirable for a feed drive system. However, it is difficult to eliminate the vibration. The most one can accomplish is to keep the vibration at a tolerable value. The existence of large values of vibration prohibits high-speed operation and this makes vibration analysis of a feed drive system necessary. A basic understanding of the underlying phenomena is vital to control these vibrations and save operations of the system.

Although the dynamic responses of problems of oscillations of beams with a moving force or attached moving masses, in which the inertia term of the riding particle is taken into account, have received much attention for many years [1–8], dynamic characteristics of these systems have not been fully clarified yet. The motion of the whole structure is usually deduced from the analysis of a single moving concentrated mass instead of a moving table with finite length. Furthermore, in most research either the velocity or the acceleration of moving mass is held to be constant.

We are concerned here with the vibration response of a feed drive system induced by a worktable with finite length that travels with high speed. A simple model, which uses

0022-460X/01/030489 + 16 $35.00/0

spring, mass and damper, has been constructed that describes the complex interaction between the moving table and the supporting structures, i.e., guide ways. This model includes the effect of friction between the table and the guide way. Moreover, important features to be carried out in the analysis include the ability to bring the table to a halt at a desired position and an arbitrary moving velocity profile for the table. The focus is placed on the vibration response caused by different velocity motion programs and it is the basis to investigate the dynamics of a feed drive system due to the motion of the moving table. Finally, numerical results of the vibration response are obtained to illustrate the theoretical predictions.

2. FORMULATION

A feed drive system is an assembly of individual units, such as servomotor, guide way, supporting structures and work table. A work table is mounted on a supporting structure with suitable guide ways and a feed screw is used to impart motion to the work table. A feed drive is now considered from the point of view of its dynamic characteristics, therefore it may be considered as a multi-mass vibrator. Consider that a table of finite length l is travelling on a supporting structure with variable speed as shown in Figure 1. Interfaces of individual components are modelled using springs and dampers. Especially, the damping capacity of the table is mainly produced in the contacting surface (e.g., guide way) and the equivalent coefficient of viscous damping is assumed to be independent of the moving speed of the table [9]. The notations used in Figure 1 to describe the motion of the feed drive system when the table is moving are listed in Appendix A.

In Figure 1, **i** and **j** are unit vectors in the non-rotating x–y frame, whereas **t** and **n** are the directions tangential and normal to the supporting structure. The co-ordinates, h_l, h_3, h_5, θ_M and θ_B are used to describe the motions of the system. In order to derive the governing equations of motion, the velocity and acceleration of the table should be found first. The velocity $\mathbf{V}_M$ of the mass center of the table as denoted by P is given by

$$\mathbf{V}_M = \mathbf{V}_B + \mathbf{V}_{rel} + \dot{\boldsymbol{\theta}}_B \times \mathbf{QP}, \tag{1}$$

where vectors are represented by boldfaced letters, the subscript M stands for the table, the subscript B denotes the supporting structure, a dot superscript means a time derivative, $\mathbf{V}_B$ is

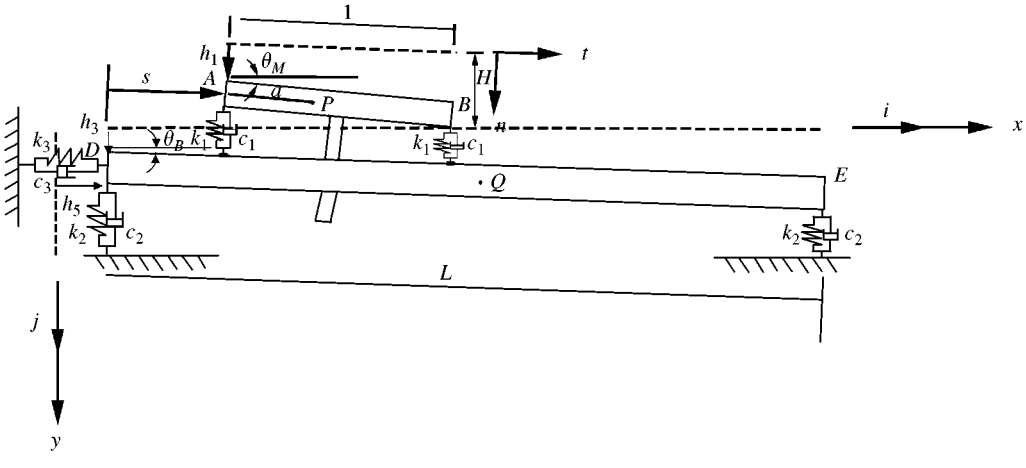

Figure 1. System configuration while the table is moving.

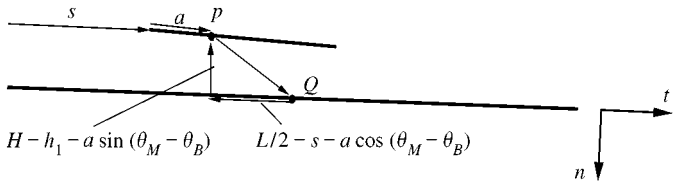

Figure 2. Geometry of position vector **QP**.

the velocity of the mass center of the supporting structure, $\mathbf{V}_{rel}$ is the table velocity relative to the supporting structure and **QP** is the position vector directed from P to Q. The relative velocity $\mathbf{V}_{rel}$ is expressed as

$$\mathbf{V}_{rel} = V_{reli}\mathbf{i} + V_{relj}\mathbf{j}, \tag{2}$$

where V_{reli} and V_{relj} are Cartesian components of the relative velocity given by

$$\begin{aligned} V_{relj} = {} & (\dot{h}_1 + a(\dot{\theta}_M - \dot{\theta}_B)\cos(\theta_M - \theta_B))\cos\theta_B \\ & + (V_{Mt} - a(\dot{\theta}_M - \dot{\theta}_B)\sin(\theta_M - \theta_B))\sin\theta_B, \end{aligned} \tag{3}$$

$$\begin{aligned} V_{reli} = {} & -(\dot{h}_1 + a(\dot{\theta}_M - \dot{\theta}_B)\cos(\theta_M - \theta_B))\sin\theta_B \\ & + (V_{Mt} - a(\dot{\theta}_M - \dot{\theta}_B)\sin(\theta_M - \theta_B))\cos\theta_B. \end{aligned} \tag{4}$$

Note that V_{Mt} is the table moving speed tangential to the supporting structure and it is given by a known motion program. The position vector **QP** as shown in Figure 2 is expressed as

$$\mathbf{QP} = QP_i\mathbf{i} + QP_j\mathbf{j}, \tag{5}$$

where

$$QP_i = (H - h_1 - a\sin(\theta_M - \theta_B))\sin\theta_B - \left(\frac{L}{2} - s - a\sin(\theta_M - \theta_B)\right)\cos\theta_B, \tag{6}$$

$$QP_j = -(H - h_1 - a\sin(\theta_M - \theta_B))\cos\theta_B - \left(\frac{L}{2} - s - a\sin(\theta_M - \theta_B)\right)\sin\theta_B. \tag{7}$$

The acceleration $\mathbf{a}_M$ of the mass center P is expressed as

$$\mathbf{a}_M = \mathbf{a}_B + \mathbf{a}_{rel} + \ddot{\boldsymbol{\theta}}_B \times \mathbf{QP} + \dot{\boldsymbol{\theta}}_B \times (\dot{\boldsymbol{\theta}}_B \times \mathbf{QP}) + 2\dot{\boldsymbol{\theta}}_B \times \mathbf{V}_{rel}, \tag{8}$$

where a double dot superscript means a second derivative with respect to time, $\mathbf{a}_B$ is the acceleration of the supporting structure and $\mathbf{a}_{rel}$ is the table acceleration relative to the supporting structure. Letting $\sin\theta \doteqdot \theta$ and $\cos\theta \doteqdot 1$ for small angles, furthermore, neglecting its associated high-order terms, θ_M^2, θ_B^2 and $\theta_M\theta_B$, the velocity and acceleration of the mass

center P relative to the supporting structure are approximated by

$$\mathbf{V}_{rel} = [-\dot{h}_1\theta_B + V_{Mt} - a(\dot{\theta}_M - \dot{\theta}_B)\theta_M]\mathbf{i} + [\dot{h}_1 + a(\dot{\theta}_M - \dot{\theta}_B) + V_{Mt}\theta_B]\mathbf{j}, \tag{9}$$

$$\begin{aligned}\mathbf{a}_{rel} = {} & [-\ddot{h}_1\theta_B - a(\ddot{\theta}_M - \ddot{\theta}_B)\theta_M + a_{Mt} - \dot{h}_1\dot{\theta}_B - V_{Mt}\dot{\theta}_B\theta_B - a(\dot{\theta}_M - \dot{\theta}_B)\dot{\theta}_M)]\mathbf{i} \\ & + [\ddot{h}_1 + a(\ddot{\theta}_M - \ddot{\theta}_B) + a_{Mt}\theta_B - \dot{h}_1\dot{\theta}_B\theta_B + V_{Mt}\dot{\theta}_B - a(\dot{\theta}_M - \dot{\theta}_B)\dot{\theta}_M\theta_M]\mathbf{j},\end{aligned} \tag{10}$$

where a_{Mt} is the table acceleration tangential to the supporting structure and is given by a motion program. Although the angles, θ_B and θ_M are assumed to be small, it does not imply that the associated angular velocity and angular acceleration are small, correspondingly. The acceleration of the mass center Q of the supporting structure is expressed as

$$\mathbf{a}_B = \left[\ddot{h}_5 - \frac{L}{2}\ddot{\theta}_B\theta_B - \frac{L}{2}\dot{\theta}_B^2\right]\mathbf{i} + \left[\ddot{h}_3 + \frac{L}{2}\ddot{\theta}_B - \frac{L}{2}\dot{\theta}_B^2\theta_B\right]\mathbf{j}. \tag{11}$$

Substituting equations (6), (7), (9) and (10) into equation (8), the Cartesian components of the acceleration of the table, a_{Mx} and a_{Mx} are

$$\begin{aligned}a_{Mx} = {} & a_{Mt} - 3V_{Mt}\dot{\theta}_B\theta_B - 3\dot{h}_1\dot{\theta}_B + a\dot{\theta}_B^2 - s\dot{\theta}_B^2 - H\dot{\theta}_B^2\theta_B + h_1\dot{\theta}_B^2\theta_B \\ & - a\dot{\theta}_B^2\theta_B^2 + a\dot{\theta}_B^2\theta_B\theta_M - a\dot{\theta}_B\dot{\theta}_M - a\dot{\theta}_M^2 - \ddot{h}_1\theta_B + \ddot{h}_5 + H\ddot{\theta}_B \\ & - h_1\ddot{\theta}_B - s\ddot{\theta}_B\theta_B - a\ddot{\theta}_M\theta_M,\end{aligned} \tag{12}$$

$$\begin{aligned}a_{My} = {} & a_{Mt}\theta_B + 3V_{Mt}\dot{\theta}_B - 3\dot{h}_1\dot{\theta}_B\theta_B + H\dot{\theta}_B^2 - h_1\dot{\theta}_B^2 - s\dot{\theta}_B^2\theta_B + a\dot{\theta}_B^2\theta_M \\ & - a\dot{\theta}_B\dot{\theta}_M\theta_M - a\dot{\theta}_M^2\theta_M + \ddot{h}_1 + \ddot{h}_3 + s\ddot{\theta}_B + H\ddot{\theta}_B\theta_B - h_1\ddot{\theta}_B\theta_B \\ & + a\ddot{\theta}_B\theta_B^2 - a\ddot{\theta}_B\theta_B\theta_M + a\ddot{\theta}_M.\end{aligned} \tag{13}$$

The unknowns in equations (12) and (13) are h_1, h_3, θ_B, θ_M and their associated time derivatives. In spite of the simplicity of the model, the mathematical analysis for its behavior is rather complicated due to the presence of the convective acceleration. The equations governing the motion of the system can be derived from the dynamic equilibrium of forces and momenta. Dynamic equilibrium from the free-body diagram of the table shown in Figure 3 yields the following equations:

$$(f_1 + f_2 + f_3 + f_4)\sin\theta_B - \mu(f_1 + f_2 + f_3 + f_4)\cos\theta_B + f_p - f_{cx} = Ma_{Mx}, \tag{14}$$

$$-(f_1 + f_2 + f_3 + f_4)\cos\theta_B - \mu(f_1 + f_2 + f_3 + f_4)\sin\theta_B + f_{cy} + Mg = Ma_{My}, \tag{15}$$

$$\begin{aligned}& (f_1 + f_2)\cos(\theta_M - \theta_B)a + f_{cy}(c - a)\cos\theta_M - (f_3 + f_4)\cos(\theta_M - \theta_B)b \\ & + \mu(f_1 + f_2)(H - h_1 - a\sin(\theta_M - \theta_B)) - f_{cx}(H_W\cos\theta_M - (c - a)\sin\theta_M) \\ & + \mu(f_3 + f_4)(H - h_1 - (a + b)\sin(\theta_M - \theta_B)) - f_P h_P = I_M\ddot{\theta}_M,\end{aligned} \tag{16}$$

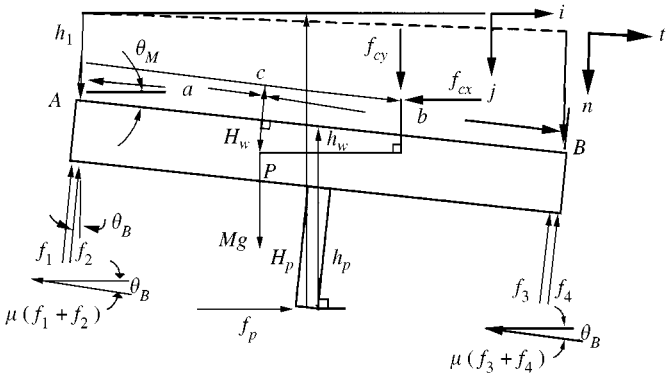

Figure 3. Free-body diagram of the table.

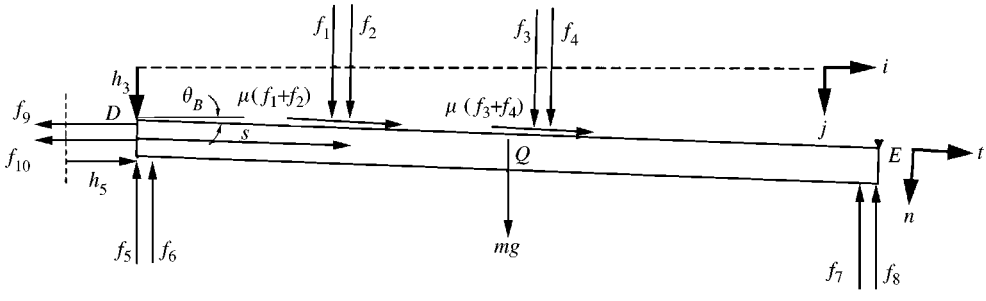

Figure 4. Free-body diagram of the supporting structure.

The notations used in equations (14–16) and Figure 3 are listed in Appendix A. Forces from the interfaces are given by

$$f_1 = k_1 h_1, \tag{17a}$$

$$f_2 = c_1 \dot{h}_1, \tag{17b}$$

$$f_3 = k_1 + (a+b)(\theta_M - \theta_B)], \tag{17c}$$

$$f_4 = c_1[\dot{h}_1 + (a+b)(\dot{\theta}_M - \dot{\theta}_B)]. \tag{17d}$$

Dynamic equilibrium from the free-body diagram of the supporting structure shown in Figure 4 yields the following equations:

$$-f_9 - f_{10} - (f_1 + f_2 + f_3 + f_4)\sin\theta_B + \mu(f_1 + f_2 + f_3 + f_4)\cos\theta_B = ma_{Bx}, \tag{18}$$

$$(f_1 + f_2 + f_3 + f_4)\cos\theta_B - (f_5 + f_6 + f_7 + f_8) + \mu(f_1 + f_2 + f_3 + f_4)\sin\theta_B + mg = ma_{By}, \tag{19}$$

$$((f_5 + f_6) - (f_7 + f_8))\cos\theta_B \frac{L}{2} - (f_1 + f_2)\left(\frac{L}{2} - s\right) + (f_3 + f_4)\left(s + a + b - \frac{L}{2}\right)$$

$$-(f_9 + f_{10})\sin\theta_B \frac{L}{2} = I_B \ddot{\theta}_B, \tag{20}$$

where m is the mass of the supporting structure and I_B is the mass moment of inertia of the supporting structure. Forces from interfaces are given by

$$f_5 = k_2 h_3, \tag{21a}$$

$$f_6 = c_2 \dot{h}_3, \tag{21b}$$

$$f_7 = k_2(h_3 + L\theta_B), \tag{21c}$$

$$f_8 = c_2(\dot{h}_3 + L\dot{\theta}_B), \tag{21d}$$

$$f_9 = k_3 h_5, \tag{21e}$$

$$f_{10} = c_3 \dot{h}_5. \tag{21f}$$

The dynamic behavior of a feed drive system is determined by a set of non-linear, second order differential equations (12–21) with unknowns, h_1, h_3, θ_B, θ_M and f_p. The numerical scheme of the system is obtained by introducing state vectors into the equations of motion and hence reducing these equations to the first order state equations with specified initial conditions which are solved by using the Runge–Kutta method [10].

2.2. NON-DIMENSIONALIZATION

It is convenient to present numerical results in terms of dimensionless parameters that are defined as follows:

$$\hat{M} = \frac{M}{m}, \quad \hat{I}_M = \frac{I_M}{mL^2}, \quad \hat{I}_B = \frac{I_B}{mL^2}, \quad \hat{s} = \frac{s}{L},$$

$$\hat{l} = \frac{a+b}{L}, \quad \hat{a} = \frac{a}{L}, \quad \hat{b} = \frac{b}{L}, \quad \hat{H} = \frac{H}{L},$$

$$\hat{c} = \frac{c}{L}, \quad \hat{H}_P = \frac{H_P}{L}, \quad \hat{h}_P = \frac{h_P}{L}, \quad \hat{H}_W = \frac{H_W}{L},$$

$$\hat{h}_W = \frac{h_W}{L}, \quad \hat{k}_1 = \frac{k_1}{k_2}, \quad \hat{k}_3 = \frac{k_3}{k_2}, \quad \hat{k}_3 = \frac{k_3}{k_2},$$

$$\hat{\zeta}_1 = \frac{c_1}{\sqrt{k_2 m}}, \quad \hat{\zeta}_2 = \frac{c_2}{\sqrt{k_2 m}}, \quad \hat{\zeta}_3 = \frac{c_3}{\sqrt{k_2 m}}, \quad \hat{t}_1 = \frac{t}{\sqrt{m/k_2}},$$

$$\hat{g} = \frac{m}{k_2 L} g, \quad \hat{a}_{Mt} = \frac{m}{k_2 L} a_{Mt}, \quad \hat{V}_{Mt} = \frac{1}{\sqrt{k_2/mL}} V_{Mt}, \quad \hat{h}_1 = \frac{h_1}{L},$$

$$\hat{h}_3 = \frac{h_3}{L}, \quad \hat{h}_5 = \frac{h_5}{L}, \quad \dot{\hat{h}}_1 = \frac{1}{\sqrt{k_2/mL}} \dot{h}_1, \quad \dot{\hat{h}}_3 = \frac{1}{\sqrt{k_2/mL}} \dot{h}_3,$$

$$\dot{\hat{h}}_5 = \frac{1}{\sqrt{k_2/mL}}\dot{h}_5, \quad \ddot{\hat{h}}_1 = \frac{m}{k_2 L}\ddot{h}_1, \quad \ddot{\hat{h}}_3 = \frac{m}{k_2 L}\ddot{h}_3, \quad \ddot{\hat{h}}_5 = \frac{m}{k_2 L}\ddot{h}_5,$$

$$\dot{\hat{\theta}}_M = \sqrt{\frac{m}{k_2}}\,\dot{\theta}_M, \quad \ddot{\hat{\theta}}_M = \frac{m}{k_2}\ddot{\theta}_M, \quad \dot{\hat{\theta}}_B = \sqrt{\frac{m}{k_2}}\,\dot{\theta}_B, \quad \ddot{\hat{\theta}}_B = \frac{m}{k_2}\ddot{\theta}_B,$$

$$\hat{f}_P = \frac{1}{k_2 L} f_P, \quad \hat{f}_{cx} = \frac{1}{k_2 L} f_{cx}, \quad \hat{f}_{cy} = \frac{1}{k_2 L} f_{cy}. \tag{22}$$

Substitution of dimensionless parameters into equations (12–21) gives the dimensionless equations of motion

$$(\hat{f}_1 + \hat{f}_2 + \hat{f}_3 + \hat{f}_4)\hat{\theta}_B - \mu(\hat{f}_1 + \hat{f}_2 + \hat{f}_3 + \hat{f}_4) + \hat{f}_P - \hat{f}_{cx} - \hat{M}\hat{a}_{Mx} = 0, \tag{23}$$

$$-(\hat{f}_1 + \hat{f}_2 + \hat{f}_3 + \hat{f}_4) - \mu(\hat{f}_1 + \hat{f}_2 + \hat{f}_3 + \hat{f}_4)\hat{\theta}_B + \hat{f}_{cy} + \hat{M}\hat{g} - \hat{M}\hat{a}_{My} = 0, \tag{24}$$

$$\begin{aligned}(\hat{f}_1 + \hat{f}_2)\hat{a} + \hat{f}_{cy}(\hat{c} - \hat{a}) - (\hat{f}_3 + \hat{f}_4)\hat{b} + \mu(\hat{f}_1 + \hat{f}_2)(\hat{H} - \hat{h}_1 - \hat{a}(\hat{\theta}_M - \hat{\theta}_B))\\ - \hat{f}_{cx}(\hat{H}_W - (\hat{c} - \hat{a})\hat{\theta}_M) + \mu(\hat{f}_3 + \hat{f}_4)(\hat{H} - \hat{h}_1 - (\hat{a} + \hat{b})(\hat{\theta}_M - \hat{\theta}_B))\\ - \hat{f}_P\hat{h}_P - \hat{I}_M\ddot{\hat{\theta}}_M = 0,\end{aligned} \tag{25}$$

$$-\hat{f}_9 - \hat{f}_{10} - (\hat{f}_1 + \hat{f}_2 + \hat{f}_3 + \hat{f}_4)\hat{\theta}_B + \mu(\hat{f}_1 + \hat{f}_2 + \hat{f}_3 + \hat{f}_4) - \hat{m}\hat{a}_{Bx} = 0, \tag{26}$$

$$(\hat{f}_1 + \hat{f}_2 + \hat{f}_3 + \hat{f}_4) - (\hat{f}_5 + \hat{f}_6 + \hat{f}_7 + \hat{f}_8) + \mu(\hat{f}_1 + \hat{f}_2 + \hat{f}_3 + \hat{f}_4)\hat{\theta}_B + \hat{m}\hat{g} - \hat{m}\hat{a}_{By} = 0, \tag{27}$$

$$\begin{aligned}((\hat{f}_5 + \hat{f}_6) - (\hat{f}_7 + \hat{f}_8))\frac{\hat{L}}{2} - (\hat{f}_1 + \hat{f}_2)\left(\frac{\hat{L}}{2} - \hat{s}\right) + (\hat{f}_3 + \hat{f}_4)\left(\hat{s} + \hat{a} + \hat{b} - \frac{\hat{L}}{2}\right)\\ - (\hat{f}_9 + \hat{f}_{10})\hat{\theta}_B\frac{\hat{L}}{2} - \hat{I}_B\ddot{\hat{\theta}}_B = 0.\end{aligned} \tag{28}$$

3. ANALYSIS PARAMETERS

In order to evaluate the dynamic response, several parameters must be specified to illustrate some features of the theoretical results. The supporting structure and table are chosen with the following dimensionless parameters: $\hat{l} = 0{\cdot}2$, $\hat{a} = 0{\cdot}1$, $\hat{b} = 0{\cdot}1$, $\hat{c} = 0{\cdot}16$, $\hat{H} = 0{\cdot}01$, $\hat{H}_P = 0{\cdot}02$, $\hat{H}_W = 0{\cdot}016$, $\hat{I}_M = 0{\cdot}0002$, $\hat{I}_B = 0{\cdot}1$, $\hat{k}_1 = 5$, $\hat{k}_2 = 5$, $\hat{k}_3 = 5$, $\hat{c}_1 = 0{\cdot}02$, $\hat{c}_2 = 0{\cdot}02$, $\hat{c}_3 = 0{\cdot}02$, and $\hat{g} = 1 \times 10^{-6}$. Assume that there is no cutting force exerted on the table and the table initially is at rest in its static equilibrium position on the supporting structure. Then, the table is set into motion from the center, $s = 0{\cdot}4$, $\hat{t} = 0$ to the right end, $s = 0{\cdot}8$, at $\hat{t} = 80$ of the supporting structure. In order to demonstrate the effects of the table moving speed on the dynamic response of a feed drive system, several motion programs for the moving table are chosen and will be discussed in the following section.

4. NUMERICAL RESULTS AND DISCUSSION

Numerical results have been divided into three sections. The first section demonstrates the effects of motion programs of different types on the vibration response of a feed drive system. The second is a comparison of the vibration responses caused by the table that is moving with different maximum speeds. The third is an investigation of symmetrical effects of motion programs on the vibration response.

4.1. INFLUENCES OF MOTION PROGRAMS OF DIFFERENT TYPES ON THE TABLE RESPONSE

As stated before, important features to be considered in this study include the ability to bring the table to a halt at a desired position and the ability of the table to travel with an arbitrary moving velocity profile. In general, the quantitative identification of velocity profiles is necessary in a feed drive system. Different motion programs for the moving table result in different levels of vibration. In order to examine the vibration response while the table is subject to different motion programs, two velocity profiles are selected as shown in Figure 5. One of them is a motion program with a constant acceleration and a constant deceleration. Note that there exist abrupt changes in the velocities at the beginning, at the maximum speed and at the stop of the table. The other is a cycloidal motion program described by

$$V_{Mt} = \frac{v_{max}}{2}\left[1 - \cos\left(\frac{2\pi t}{T}\right)\right], \tag{29}$$

where v_{max} is the associated maximum speed of the table and T is twice of the period for the table to reach the maximum velocity. Note that there are no abrupt changes in the velocity and the acceleration either at the beginning or at the end. In both programs, the table takes

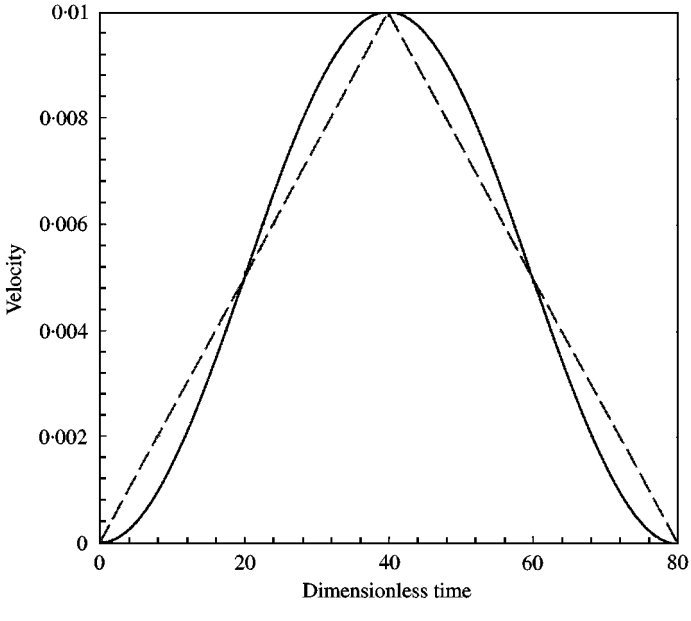

Figure 5. Different types of motion programs:——, type 1; – – –, type 4.

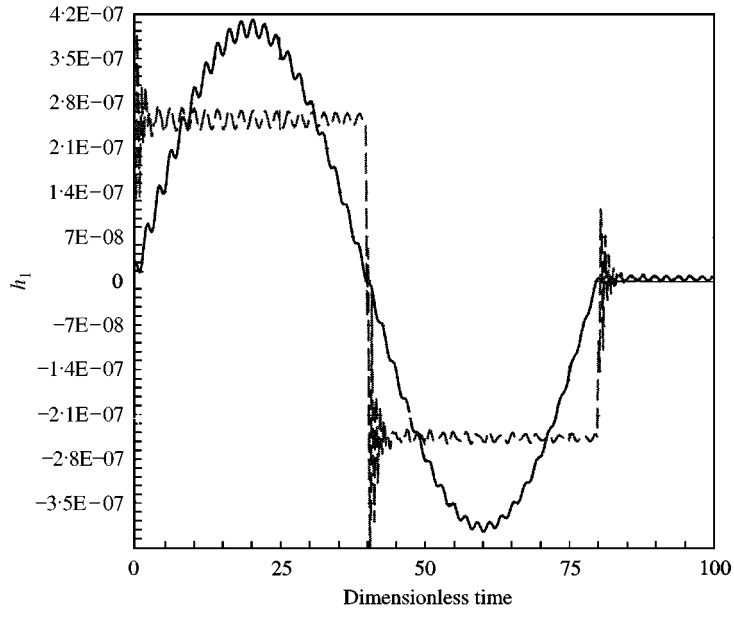

Figure 6. Vertical displacement of the table subjected to different types of motion programs: ——, type 1; – – –, type 4.

the same time to reach its maximum speed; then it moves to the right end of the supporting structure.

The vertical displacement of the table relative to the supporting structure is plotted in Figure 6. It shows that the table oscillates slowly in the vertical direction. The inertia force, which acts through the center of gravity of the table, induces a motion in rotation due to inertia coupling. When the table is travelling with the constant acceleration motion program, it is not surprising that there are severe vibrations where sudden changes in velocities occur. These abrupt changes in velocities give infinite jerks that cause intolerable vibration and lead to position inaccuracies in a feed drive system. To improve accuracy, it can often be more cost-effective to control the rate of change of acceleration than to redesign mechanical structures.

4.2. SPEED EFFECTS ON THE TABLE RESPONSE

With the increased demands in table speed, considerable vibration problems become apparent. In order to obtain a better understanding of the effects of table speed on the vibration of a feed drive system, three cycloidal motion programs are chosen as shown in Figure 7. The reason to choose cycloidal motion program is due to its simplicity. Furthermore, as stated before the dwelling conditions of a cycloidal motion program at the beginning and at the end will not create sudden changes either in the velocity or in the acceleration. Three different maximum dimensionless speeds are selected. They are 0·01, 0·02 and 0·04 denoted by dashdot, solid and dashed lines in Figure 7, respectively. The vertical displacement response of the table relative to the supporting structure is plotted in Figure 8. It shows that the table oscillates slowly in the vertical direction due to inertia forces. Furthermore, the displacement of the table relative to the supporting structure grows with an increase of its moving speed.

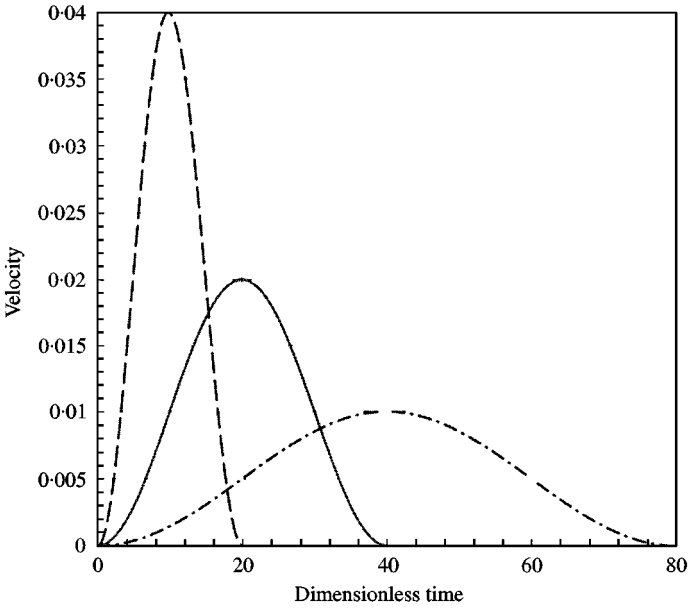

Figure 7. Velocity profiles of the table subjected to different maximum speeds: –·–·–·–, $v_{max} = 0{\cdot}01$; ——, $v_{max} = 0{\cdot}02$; – – – –, $v_{max} = 0{\cdot}04$.

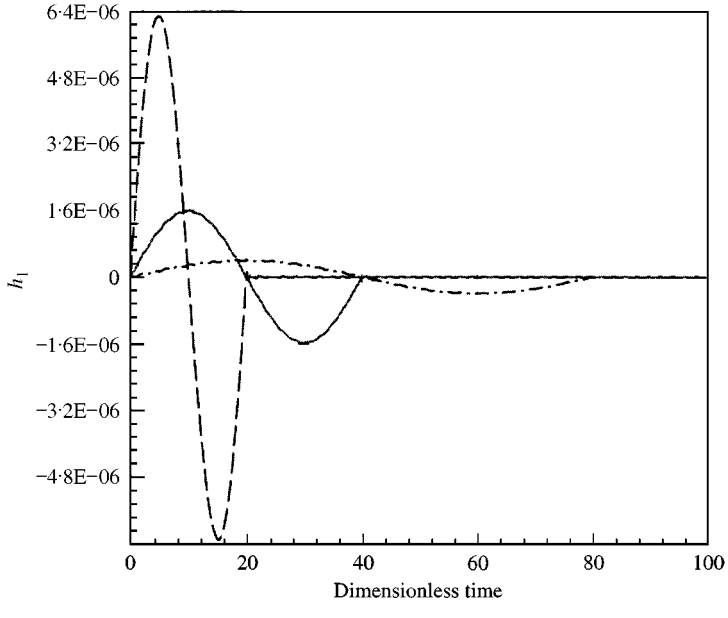

Figure 8. Vertical displacement of the table subjected to different maximum speeds. –·–·–·–, $v_{max} = 0{\cdot}01$; ——, $v_{max} = 0{\cdot}02$; – – – –, $v_{max} = 0{\cdot}04$.

If a feed drive is given higher requirements for the positioning time, as would be the case, for instance, for punch and nibbling machines or press feeder, then the vibration response after the table is brought to a halt must also be taken into consideration. Figure 9 shows similar information to that in Figure 8, except that the response is displayed after the table

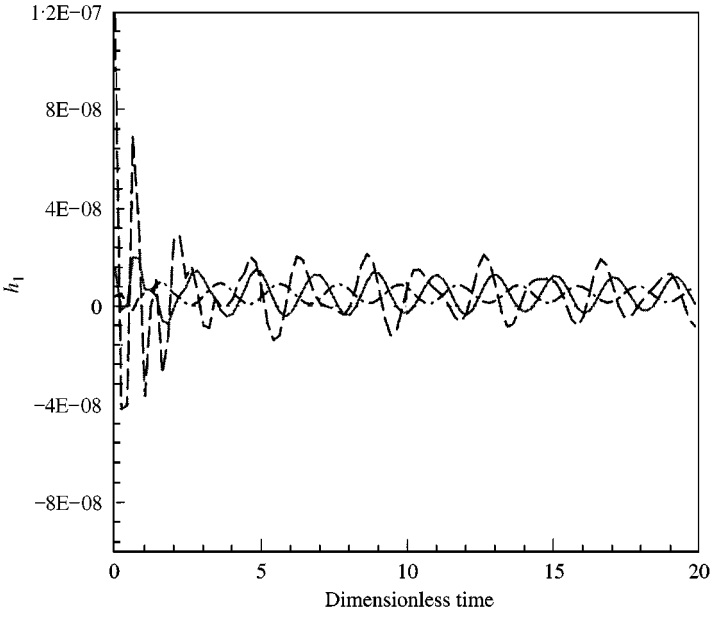

Figure 9. Vertical displacement of the table after it stops: −·−·−·−, $v_{max} = 0{\cdot}01$; ——, $v_{max} = 0{\cdot}02$; − − − −, $v_{max} = 0{\cdot}04$.

reaches the right end of the supporting structure. An excess vibration occurs barely after the moving table is brought to a halt. The displacement amplitude corresponding to the motion program $v_{max} = 0{\cdot}44$ is the largest as expected. The excess vibration is attributed to the inertia force of the table caused by the high acceleration and deceleration. From Figures 8 and 9, with an increase of the maximum speed, one may observe that the table displacement increases not only when the table is moving but also after it stops. These results showed what could be expected; however, one may find that doubling the table moving speed raises more than four times the table displacement at a moment barely after the table stops. It implies that an additional vibration absorber or a damping mechanism is necessary for a high-speed feed drive system.

4.3. SYMMETRICAL EFFECTS OF MOTION PROGRAM

Three velocity programs are chosen as shown in Figure 10. One may observe differences in these velocity curves. One of them is symmetrical with respect to the travelling time but the others are not. However, they are all cycloidal types of motion programs. Our purpose is to determine which program could be best put to work.

Figure 11 shows the vertical displacement of the table when the table is moving and Figure 12 is the displacement response after the table is brought to a halt. In both figures, the displacement responses of the table caused by the symmetrical and two asymmetric velocity profiles are denoted by solid, dashed and dashdot lines, respectively. In Figure 11, notice that the net response consists of the product of two multiplicative factors: the first being a short-wavelength oscillation and the second being a long-wavelength amplitude modulation. This phenomenon can also be found in Figure 6. As stated before, the long-wavelength oscillation shown in Figure 11 is induced by a motion in rotation due to inertia coupling. The short-wavelength oscillation results from the vibration of the

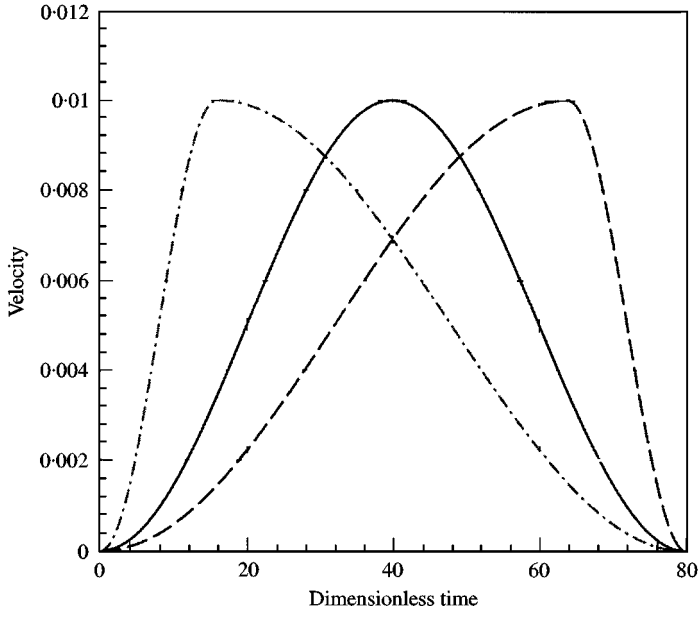

Figure 10. Symmetrical and unsymmetrical velocity profiles for a table: ——, type 1; – · – · – · –, type 2; – – – –, type 3.

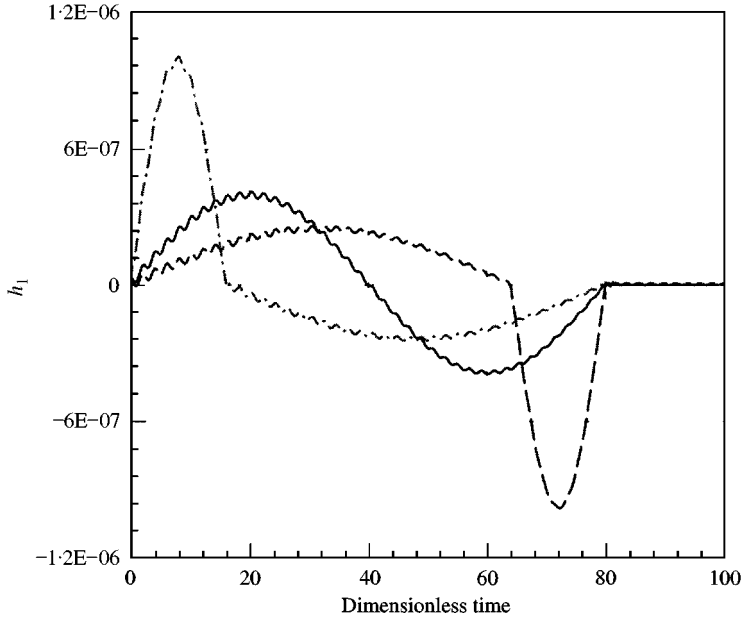

Figure 11. Vertical displacement of the table while the table is moving: ——, type 1; – · – · – · –, type 2; – – – –, type 3.

supporting structure excited by the moving table. The complete motion of the table can be described as a combination of two sinusoidal waves of different frequencies. Note that if one of the frequencies is close to, but not exactly equal to, the other frequency, the well-known phenomenon "beating" may occur. In other words if these displacements combined

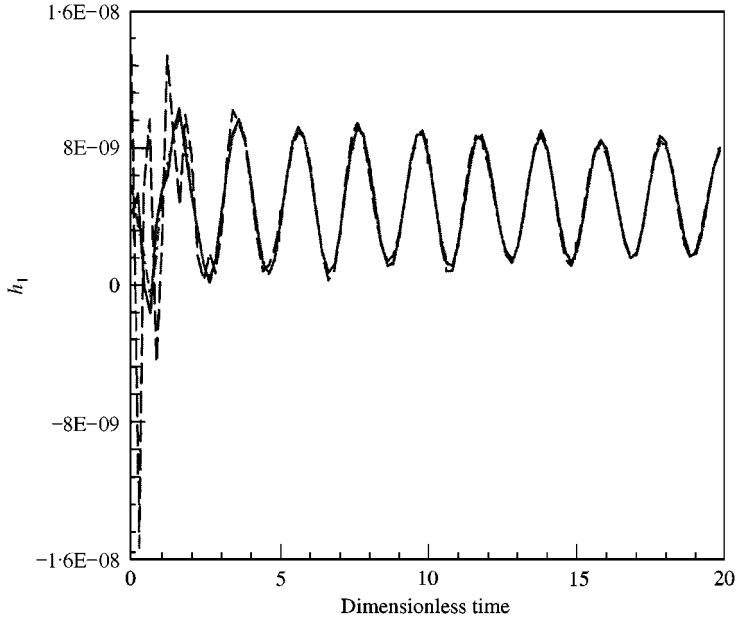

Figure 12. Vertical displacement of the table after it stops: ——, type 1; –·–·–·–, type 2; – – – –, type 3.

in-phase, the result would be

$$(\sin \omega_1 t + \sin \omega_2 t) = 2 \sin \left(\frac{\omega_1 + \omega_2}{2} \right) t \cos \left(\frac{\omega_1 - \omega_2}{2} \right) t, \tag{30}$$

where ω_1 and ω_2 represent the frequencies of two sinusoidal waves. In this kind of vibration, the amplitude builds up and then diminishes in a regular pattern, which is undesirable for a feed drive system due to an increase of the net response.

Comparing the results of the symmetrical and asymmetric velocity profiles, shown in Figures 11 and 12, it is difficult to pick a specific motion program that causes least vibration of the table. Among the responses shown in Figure 12, the profile type 3, denoted by a dashed line, displays the largest displacement barely after the table stops. This phenomenon is also attributed to the inertia effect caused by a high deceleration of the table near the end of the supporting structure.

In order to identify the influences of different velocity profiles not only on the table but also on the supporting structure. Figures 13 and 14 show the displacement response of the supporting structure in the vertical and horizontal directions. Note that friction is the main factor that causes vibration in the horizontal direction. From the general trend indicated in Figure 13 it follows that different types of motion programs have less influence on the vibration of the supporting structure in the vertical direction while the table is moving and after the table stops. However, in Figure 14, it shows that the symmetrical motion program induces less vibration in the horizontal direction for the supporting structure after the table stops. The relatively large magnitude of the displacement response in the horizontal direction caused by the asymmetric motion programs results from the relatively high acceleration and deceleration near the beginning and near the end of the travelling, respectively.

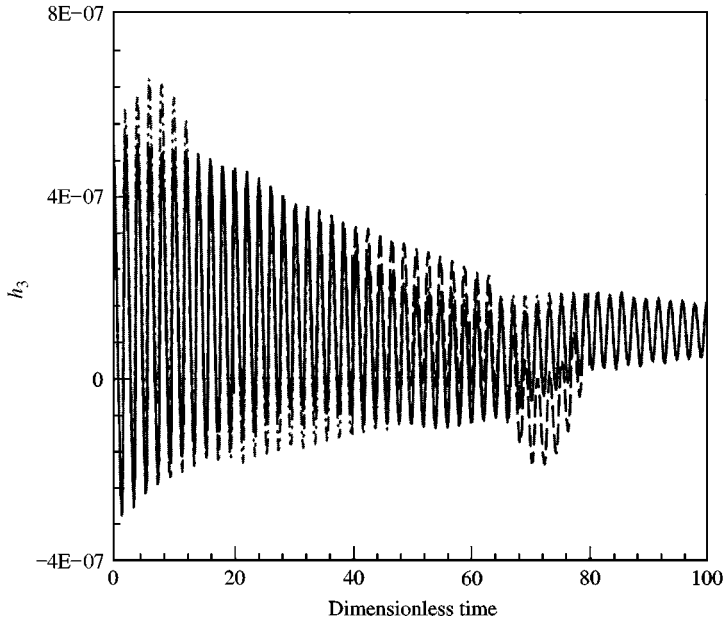

Figure 13. Vertical displacement of the supporting structure: ——, type 1; – · – · – ·–, type 2; – – – –, type 3.

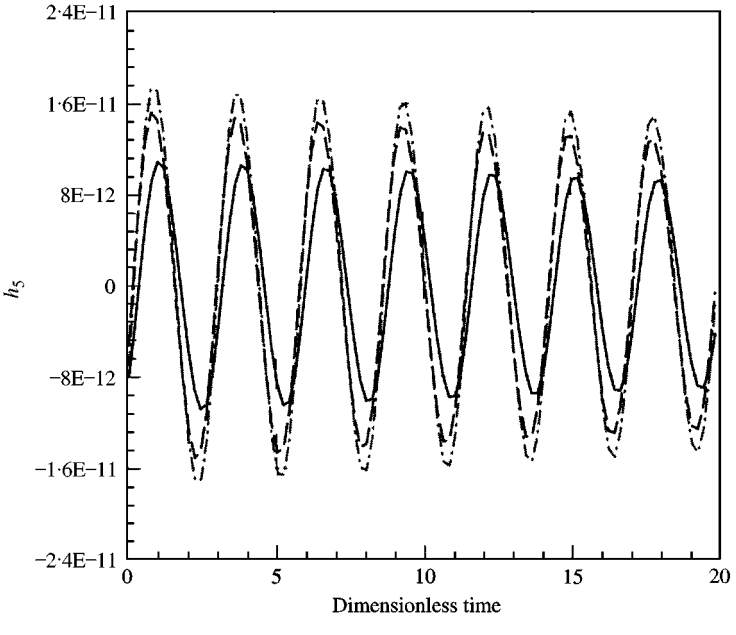

Figure 14. Horizontal displacement of the supporting structure after the table stops: ——, type 1; – · – · – ·–, type 2; – – – –, type 3.

5. CONCLUSIONS

Transient vibrations of a table with finite length that moves on a supporting structure are studied. The table is travelling with variable speed and can be brought to a halt at any

position on the supporting structure, which is found to be more practical. In spite of the simplicity of the model, the mathematical analysis of its behavior is rather complicated due to the presence of the friction and the convective acceleration. Results of this analytical study are summarized as follows:

1. Doubling the table moving speed raises more than four times the table displacement at the moment that the table stops.
2. Different motion programs for the moving table result in different levels of vibration. If accuracy needs to be maintained especially at the beginning and at the end of the table's movement, a motion program with abrupt changes in the velocity and the acceleration profiles should be avoided.
3. The symmetrical property of cycloidal motion programs has less influence on the vibration response of the supporting structure in the vertical direction. However, the symmetrical motion program leads to less vibration in the horizontal direction for the supporting structure. The relatively large displacement response caused by the asymmetric motion programs results from the relatively high acceleration and deceleration near the beginning and near the end of the travelling, respectively.
4. Although the mathematical analysis of the system behavior is rather complicated, the simulation demonstrated can easily incorporate the transient vibration during a machining process.

ACKNOWLEDGMENTS

This work was partially supported by the National Science Council of Taiwan, Republic of China under Contract No. NSC 88-2622-E-194-003.

REFERENCES

1. J. T. Jr. KENNEY 1954 *ASME Journal of Applied Mechanics* **21**, 359–364. Steady state vibrations of beam on elastic foundation for moving load.
2. J. S. LICARI and E. N. WILSON 1962 *Proceedings of the 4th U.S National Congress of Applied Mechanics*, Vol. **1**, 419–425. Dynamic response of a beam subjected to a moving force system.
3. C. E. SMITH 1964 *ASME Journal of Applied Mechanics* **31**, 29–37. Motions of a stretched string carrying a moving mass particle.
4. A. L. FLORENCE 1965 *ASME Journal of Applied Mechanics* **32**, 351–358. Travelling force on a Timoshenko beam.
5. C. R. STEELE 1967 *ASME Journal of Applied Mechanics* **34**, 111–118. The finite beam with a moving load.
6. C. R. STEELE 1968 *ASME Journal of Applied Mechanics* **35**, 481–488. The Timoshenko beam with a moving load.
7. H. D. NELSON and R. A. CONOVER 1971 *ASME Journal of Applied Mechanics* **38**, 1003–1006. Dynamic stability of a beam carrying moving masses.
8. A. A. ALEXSANDRIDIS, E. H. DOWELL and F. C. MOON 1978 *ASME Journal of Applied Mechanics* **45**, 864–870. The coupled response of a dynamic element riding on a continuously supported beam.
9. A. HIGASHIMOTO, T. WATANABE, Y. KAKINO, Y. NAKANO and H. MARUYAMA 1991 *Proceedings of CIRP Conference on PE & MS*, 567–577. Improvement of dynamic characteristics of ball screw driving system by ferromagnetic fluid damper.
10. W. H. ENRIGHT and J. D. PRYCE 1987 *ACM Transactions on Mathematical Software* **13**, 1–22. Two FORTRAN packages for assessing initial value methods.

APPENDIX A: NOMENCLATURE

a	distance from P to the left end of table
$\mathbf{a}_B$	acceleration of mass center of supporting structure
$\mathbf{a}_M$	acceleration of mass center of table
a_{Mt}	acceleration of table driven by ball screw
$\mathbf{a}_{rel}$	table acceleration relative to supporting structure
b	distance from P to the right end of table
c	distance from A to the location of cutting force and it is parallel to the table surface
c_1, c_2, c_3	damping coefficients of interfaces
f_p	thrust from ball screw
f_{cx}	cutting force in the vertical direction
f_{cy}	cutting force in the horizontal direction
h_p	vertical distance from thrust to P, $h_p = H_p - [h_1 + ((a+b)/2)\sin\theta_M]$
h_w	horizontal distance from the location of cutting force to P, $h_w = H_w\cos\theta_M - [(\mathrm{c} - \mathrm{a})\sin\theta_M]$
h_1	vertical displacement of point A relative to the supporting structure
h_3	vertical displacement of point D
h_5	horizontal displacement of point D
$\dot{h}_1$	velocity of point A relative to the supporting structure in the vertical direction
$\ddot{h}_1$	acceleration of point A relative to the supporting structure in the vertical direction
$\ddot{h}_3$	acceleration of point D in the vertical direction
$\dot{h}_5$	velocity of point D in the horizontal direction
$\ddot{h}_5$	acceleration of point D in the horizontal direction
H	vertical distance from P to the surface of supporting structure before the table is set to move
H_p	vertical distance from table before it is set into motion to the thrust f_p
H_w	distance from mass center of table P to the location of cutting force and it is normal to the table surface
I_B	mass moment of inertia of supporting structure
I_M	mass moment of inertia of table
k_1, k_2, k_3	elastic constants of interfaces
l	length of table, $= a + b$
L	length of supporting structure
m	mass of supporting structure
M	mass of table
P	mass center of table
Q	mass center of supporting structure
$\mathbf{QP}$	position vector directed from P to Q
s	distance along which the table is moving
T	period for table to reach maximum velocity
$\mathbf{V}_B$	velocity of mass center Q of supporting structure
V_{Mt}	table velocity driven by ball screw
$\mathbf{V}_M$	velocity of mass center P of table
$\mathbf{V}_{rel}$	table velocity relative to supporting structure
V_{reli}, V_{relj}	Cartesian components of the relative velocity, $\mathbf{V}_{rel}$
v_{max}	maximum speed of table
$\dot{\boldsymbol{\theta}}_B$	angular velocity of supporting structure
$\ddot{\boldsymbol{\theta}}_B$	angular acceleration of supporting structure
$\dot{\theta}_M$	angular velocity of table
$\ddot{\theta}_M$	angular acceleration of table
μ	friction coefficient